



Synthesis and evaluation of quinoxaline derivatives as potential influenza NS1A protein inhibitors

Lei You^a, Eun Jeong Cho^b, John Leavitt^c, Li-Chung Ma^d, Gaetano T. Montelione^{d,e}, Eric V. Anslyn^{a,*}, Robert M. Krug^{c,*}, Andrew Ellington^a, Jon D. Robertus^a

^a Department of Chemistry and Biochemistry, University of Texas at Austin, Austin, TX 78712, USA

^b The Institute for Drug and Diagnostic Development, University of Texas at Austin, Austin, TX 78712, USA

^c Department of Molecular Genetics and Microbiology, University of Texas at Austin, Austin, TX 78712, USA

^d Center for Advanced Biotechnology and Medicine, Department of Molecular Biology and Biochemistry, Rutgers The State University of New Jersey, Piscataway, NJ 08854, USA

^e Department of Biochemistry, Robert Wood Johnson Medical School, Piscataway, NJ 08854, USA

ARTICLE INFO

Article history:

Received 18 January 2011

Revised 10 March 2011

Accepted 11 March 2011

Available online 17 March 2011

Keywords:

Quinoxaline derivatives

NS1A protein

Influenza A virus

Fluorescence polarization

ABSTRACT

A library of quinoxaline derivatives were prepared to target non-structural protein 1 of influenza A (NS1A) as a means to develop anti-influenza drug leads. An in vitro fluorescence polarization assay demonstrated that these compounds disrupted the dsRNA–NS1A interaction to varying extents. Changes of substituent at positions 2, 3 and 6 on the quinoxaline ring led to variance in responses. The most active compounds (**35** and **44**) had IC₅₀ values in the range of low micromolar concentration without exhibiting significant dsRNA intercalation. Compound **44** was able to inhibit influenza A/Udorn/72 virus growth.

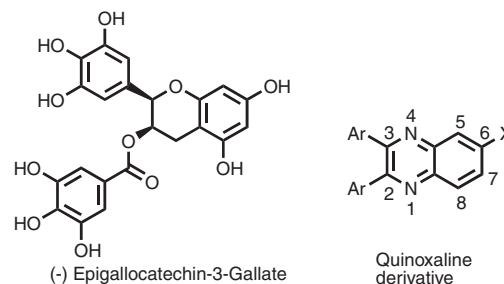
© 2011 Elsevier Ltd. All rights reserved.

Influenza viruses cause a highly contagious respiratory disease in humans. They are RNA viruses composed of three general types: influenza A, influenza B, and influenza C.¹ The type A viruses cause the most severe diseases, and as a result, are the most serious threat to human health.² The influenza A virus can be further divided into different serotypes. H1N1 caused the 2009 flu pandemic,³ and H5N1 is a current pandemic threat.⁴ Therefore, the development of small molecule based anti-influenza therapeutics continues to capture significant attention.^{5,6}

The NS1 protein,⁷ a highly conserved influenza virus encoded protein, has been identified as a potential target for antiviral development.⁸ Specifically, the double-stranded RNA (dsRNA) binding domain, comprising residues 1–73, is crucial for virus replication, and is the primary target of our work. Detailed biophysical and structural studies by high-resolution NMR and X-ray analysis revealed that the N-terminal domain of the NS1A protein forms a homodimer with a unique six-helical chain fold.⁷ There is a deep cavity at the center of dsRNA-binding surface. If a small molecule

can fit into this cavity, it can block dsRNA binding and thus inactivate the NS1 protein.

(–)-Epigallocatechin-3-gallate (EGCG)⁹ was identified to inhibit NS1A through high-throughput screening. EGCG and its derivatives¹⁰ display a broad range of biological activities.¹¹ In an effort to design and synthesize structurally simple molecules targeting NS1A protein,



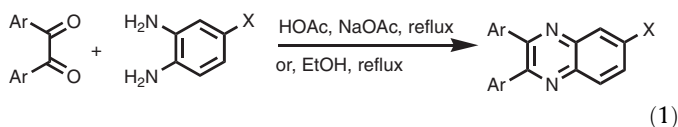
we turned our attention into the quinoxaline scaffold, which can be rapidly constructed. Quinoxalines, an important class of heterocycles, are components of several biologically active compounds.¹² Quinoxaline and EGCG share structural similarities: a bicyclic ring and the potential for substitution with polar groups on the ring.

* Corresponding authors. Tel.: +1 512 471 0068; fax: +1 512 471 7791 (E.V.A.); tel.: +1 512 232 5563; fax: +1 512 232 5565 (R.M.K.).

E-mail addresses: anslyn@austin.utexas.edu (E.V. Anslyn), rkrug@mail.utexas.edu (R.M. Krug).

Here, we report a structure–activity relationship (SAR) study with quinoxaline analogs targeting the NS1A protein.

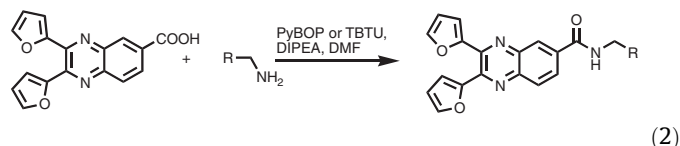
A library of 46 compounds were designed and synthesized. While keeping the quinoxaline core, various aromatic residues, such as 4-methoxyphenyl, 4-hydroxyphenyl, 2-furyl, and 2-pyridyl, were incorporated into positions 2 and 3, and different substituents were also placed in position 6. In general, 2,3-disubstituted quinoxalines were prepared by condensation of 1,2-diketones and *o*-phenylenediamine derivatives in refluxing EtOH or HOAc/NaOAc (Eq. 1).¹²



For demethylation of the methoxyphenyl substituted derivatives, many conditions were tested, including HBr/HOAc, BBr₃/CH₂Cl₂, and EtSNa/DMF. For 3-methoxyphenyl and 4-methoxyphenyl substituted quinoxalines, treatment with EtSNa in refluxing DMF afforded the corresponding 3-hydroxyphenyl and 4-hydroxyphenyl derivatives when either H or OMe was in position 6. When electron-withdrawing groups, such as COOH and NO₂, were in position 6 of quinoxalines, demethylation of 3,3'-dimethoxybenzil or 4,4'-dimethoxybenzil was achieved utilizing 48% HBr in HOAc under refluxing conditions, prior to condensation with *o*-phenylenediamine derivatives (Scheme 1).

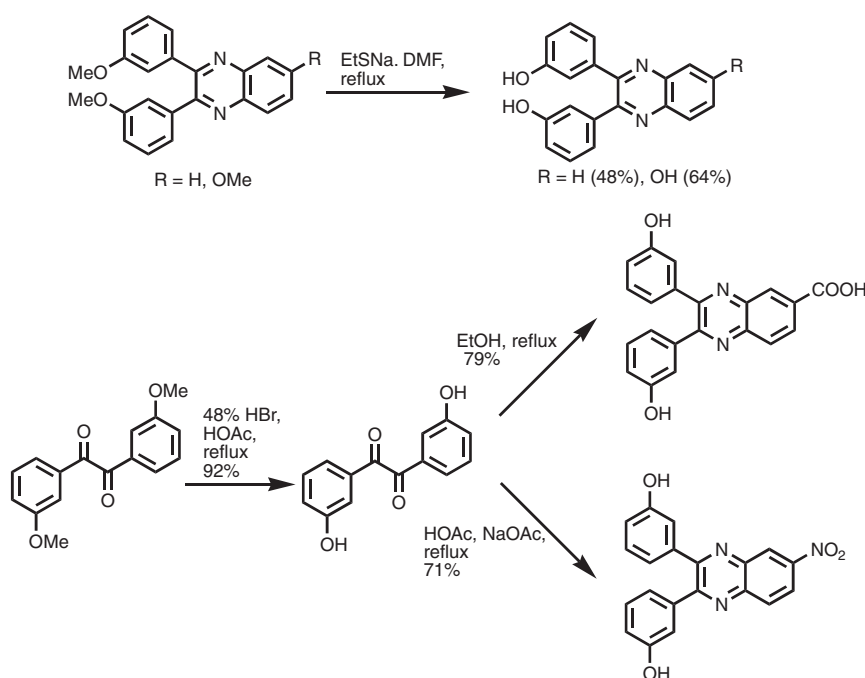
Several of the 1,2-diketones we used in (Eq. 1) are not readily available. For example, 2,2'-dimethoxybenzil was prepared from *o*-anisaldehyde using Pinacol coupling followed by oxidation.¹³ Benzoin condensation of piperonal followed by oxidation afforded 3,4,3',4'-bis(methylenedioxy)-benzil (Scheme 2). Condensation with these 1,2-phenylenediamines was done as described above. However, attempts to deprotect the catechol using either BBr₃/CH₂Cl₂ or EtSNa/DMF afforded a complicated mixture.

In addition, 2,3-furyl-quinoxaline-6-carboxylic acid was coupled with various amines using PyBOP or TBTU as a coupling reagent and DIPEA as a base to afford a library of amide substituted quinoxaline analogs (Eq. 2).

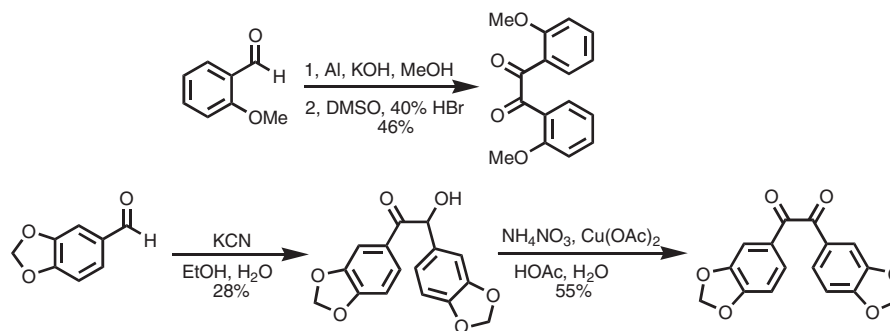


In order to examine whether the quinoxaline analogues can disrupt the dsRNA binding to NS1A protein, an *in vitro* fluorescence polarization-based binding assay (FP assay)¹⁴ was employed. In this assay, a carboxyfluorescein-labeled dsRNA (FAM-dsRNA) was used as a signaling probe. In detail, when FAM-dsRNA binds to the NS1A protein, the mobility of the fluorophore (FAM) decreases and as a result, the fluorescence polarization increases. The addition of potential NS1A inhibitors targeting the dsRNA-binding domain will displace the FAM-dsRNA from NS1A and lead to a decrease of fluorescence polarization. The data were reported as % binding at 50 μM, where a higher percentage represents stronger activity in breaking the dsRNA–NS1A interaction. A similar FP based assay to probe dsRNA intercalation of the quinoxaline derivatives was utilized as a control experiment, because targeting NS1A instead of dsRNA was desired. The data were reported as % intercalation at 50 μM, and (+) sign means intercalating to the dsRNA while (–) sign means denaturation of the dsRNA to ssRNAs. All assays were run in duplicates, and data were averaged. The compounds with high % binding at 50 μM and low % intercalation at 50 μM were subjected to further studies.

We first set out to explore SARs of 2,3,6-substituted quinoxaline derivatives, and the results are shown in Table 1. Substitution at positions 2 and 3 on the quinoxaline core had the most significant impact on the activity. Compounds with bis-2-furyl substitutions (27–30) were the most potent. Replacements of the furyl residue with methoxyphenyl (1–12), phenol (13–22), 3,4-(methylenedioxy)phenyl (23–25), or 2-pyridyl groups (31–33), reduced the activity. Compounds with phenol substitution (13–22) generally showed improved activity compared to the corresponding compounds with methoxyphenyl substitution (1–12). For bis-2-furyl substituted quinoxaline derivatives, substitution at position 6 also played an important role in the biological activity. Compounds 27,

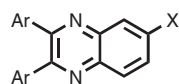


Scheme 1.



Scheme 2.

Table 1
Activities of 2,3,6-substituted quinoxaline derivatives



Compound	Ar	X	% Binding at 50 μM	% Intercalation at 50 μM
1	2-OMe-Ph-	H	5.0	-6.7
2	2-OMe-Ph-	OMe	4.4	-5.0
3	2-OMe-Ph-	COOH	2.8	-2.5
4	2-OMe-Ph-	NO ₂	6.7	-3.7
5	3-OMe-Ph-	H	1.4	-6.0
6	3-OMe-Ph-	OMe	7.2	-8.4
7	3-OMe-Ph-	COOH	9.1	-4.4
8	3-OMe-Ph-	NO ₂	1.5	1.9
9	4-OMe-Ph-	H	0.5	1.4
10	4-OMe-Ph-	OMe	1.8	5.7
11	4-OMe-Ph-	COOH	4.5	-4.8
12	4-OMe-Ph-	NO ₂	-19.7	112.7
13	2-OH-Ph-	H	-0.9	-1.0
14	2-OH-Ph-	OH	10.9	0.9
15	3-OH-Ph-	H	10.9	-4.8
16	3-OH-Ph-	OH	25.0	18.2
17	3-OH-Ph-	COOH	28.7	-3.4
18	3-OH-Ph-	NO ₂	42.8	-15.8
19	4-OH-Ph-	H	10.2	8.5
20	4-OH-Ph-	OH	38.8	29.5
21	4-OH-Ph-	COOH	13.3	-7.7
22	4-OH-Ph-	NO ₂	19.5	-32.0
23 ¹⁵	3,4-O,O-CH ₂ -Ph-	H	1.5	7.9
24	3,4-O,O-CH ₂ -Ph-	COOH	23.2	-4.8
25	3,4-O,O-CH ₂ -Ph-	NO ₂	56.6	24.4
26	2-Furyl-	H	7.3	-23.7
27	2-Furyl-	OMe	54.3	-3.2
28	2-Furyl-	COOH	60.9	5.8
29	2-Furyl-	COOMe	76.0	-12.3
30	2-Furyl-	NO ₂	25.5	25.9
31	2-Pyridyl-	H	-3.1	2.3
32	2-Pyridyl-	COOH	15.7	2.9
33	2-Pyridyl-	NO ₂	7.8	-5.6

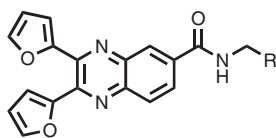
28 and **29** exhibited significantly higher activity than **26**, which has a hydrogen atom at position 6.

Next, we prepared a library based on compound **28**, and the results are listed in Table 2. Keeping 2-furyl at positions 2 and 3, phenyl groups with various substitution or heterocycles were incorporated into position 6 through an amide linker. The compounds showing the most potency were **35** and **44**, with 3-methoxyphenyl and 2-furyl at position 6, respectively. Their percentage binding at 50 μM is 79.5 ± 1.5 and 74.0 ± 1.4 μM for **44** and **35**, respectively, which is comparable to that of EGCG (89.0 ± 11.4 μM). Replacement of 3-methoxyphenyl with other methoxy substituted phenyl groups (**34**, **36–38**), fluorophenyl (**39–41**), or phenyl 4-methyl ester (**42**) resulted in reduced activity.

2-Pyridyl (**43**) substitution also decreased the biological activity. Replacement of 2-furyl with 2-thenyl (**45**) was not tolerated. An aliphatic 2-furyl mimic, glycine methyl ester derivative (**46**), showed decreased activity. The four compounds with the highest percentage binding at 50 μM were further studied in dose dependent FP assay. They have the following IC₅₀ (μM): 74.8 (**29**), 6.2 (**35**), 43.3 (**43**) and 3.5 (**44**). None of these four compounds showed significant dsRNA interference.

We then set out to explore the biological activity of the most potent compound (**44**) identified from the in vitro assay described above. Viral growth was assayed using MDCK cells infected with influenza A/Udorn/72 virus. Figure 1 shows the single cycle growth curve at MOI (multiplicity of infection) 5 (top panel) and multiple

Table 2
Activities of amide derivatives of compound 28



Compound	R	% Binding at 50 μ M	% Intercalation at 50 μ M
34	2-OMe-Ph-	29.5	-17.7
35	3-OMe-Ph-	74.0	4.5
36	4-OMe-Ph-	44.0	7.6
37	3,4-(OMe) ₂ -Ph-	39.5	5.6
38	3,4,5-(OMe) ₃ -Ph-	53.6	-4.7
39	2-F-Ph-	11.6	-11.3
40	3-F-Ph-	13.6	-11.6
41	4-F-Ph-	49.0	6.3
42	4-COOMe-Ph-	47.9	8.8
43	2-Pyridyl-	64.7	-9.6
44	2-Furyl-	79.5	5.9
45	2-Thenyl-	8.2	-10.5
46	COOMe	26.7	-27.9

effectiveness of inhibition after 37 h (bottom panel). Although these are qualitative experiments, they demonstrate the antiviral potential of those quinoxaline derivatives.

In conclusion, we have explored preliminary structure–activity relationships (SARs) for a library of quinoxaline derivatives targeting the NS1A protein for the development of anti-influenza therapeutics. Those quinoxaline derivatives were designed to mimic (–)-epigallocatechin-3-gallate, a hit identified by high-throughput screening. In vitro fluorescence polarization experiments showed that these compounds can bind to NS1A to disrupt the NS1A–dsRNA interaction. Substitution at positions 2 and 3 on the quinoxaline core played an important role, with 2-furyl being the best among those investigated. Substitution at position 6 was also crucial. Compounds 35 and 44 were the most potent, with an IC₅₀ of 6.2 and 3.5 μ M, respectively. The dsRNA intercalation experiments indicated that both 35 and 44 do not inhibit NS1A–dsRNA interactions by interfering with dsRNA, but likely function by binding to the NS1A dsRNA-binding domain itself. Results from a cell assay demonstrated that compound 44 was able to inhibit influenza A virus growth. Detailed structural analysis and optimization are currently ongoing.

Acknowledgments

We thank the National Institutes of Health (U01 AI074497) and The Texas Institute for Drug and Diagnostic Development for support of this work.

Supplementary data

Supplementary data associated with this article can be found, in the online version, at doi:10.1016/j.bmcl.2011.03.042.

References and notes

- Lagoja, I. M.; De Clercq, E. *Med. Res. Rev.* **2008**, *28*, 1.
- Taubenberger, J. K.; Morens, D. M. *Annu. Rev. Pathol. Mech. Dis.* **2008**, *3*, 499.
- Bautista, E.; Chotpitayasonondh, T.; Gao, Z.; Harper, S. A.; Shaw, M.; Uyeki, T. M.; Zaki, S. R.; Hayden, F. G.; Hui, D. S.; Kettner, J. D.; Kumar, A.; Lim, M.; Shindo, N.; Penn, C.; Nicholson, K. G. *N. Eng. J. Med.* **2010**, *362*, 1708.
- Abdel-Ghafar, A.-N.; Chotpitayasonondh, T.; Gao, Z.; Hayden, F. G.; Hien, N. D.; de Jong, M.; Naghdaliyev, A.; Peiris, J. S. M.; Shindo, N.; Soeroso, S.; Uyeki, T. M. *N. Eng. J. Med.* **2008**, *358*, 261.
- De Clercq, E. *Nat. Rev. Drug Disc.* **2006**, *5*, 1015.
- Das, K.; Aramini, J. M.; Ma, L.-C.; Krug, R. M.; Arnold, E. *Nat. Struct. Mol. Biol.* **2010**, *17*, 530.
- (a) Chien, C.; Tejero, R.; Huang, Y.; Zimmerman, D. E.; Rios, C. B.; Krug, R. M.; Montelione, G. T. *Nat. Struct. Mol. Biol.* **1997**, *4*, 891; (b) Liu, J.; Lynch, P. A.; Chien, C.; Montelione, G. T.; Krug, R. M.; Berman, H. M. *Nat. Struct. Mol. Biol.* **1997**, *4*, 896; (c) Min, J.-Y.; Krug, R. M. *Proc. Natl. Acad. Sci.* **2006**, *103*, 7100; (d) Hale, B. G.; Randall, R. E.; Ortin, J.; Jackson, D. J. *Gen. Virol.* **2008**, *89*, 2359; (e) Yin, C.; Khan, J. A.; Swapna, G. V. T.; Ertekin, A.; Krug, R. M.; Tong, L.; Montelione, G. T. *J. Biol. Chem.* **2007**, *282*, 20584.
- (a) Fernandez-Sesma, A. *Infect Disord. Drug Targets* **2007**, *7*, 336; (b) Krug, R. M.; Aramini, J. M. *Trends Pharmacol. Sci.* **2009**, *30*, 269; (c) Basu, D.; Walkiewicz, M. P.; Frieman, M.; Baric, R. S.; Auble, D. T.; Engel, D. A. *J. Virol.* **2009**, *83*, 1881; (d) Walkiewicz, M. P.; Basu, D.; Jablonski, J. J.; Geysen, H. M.; Engel, D. A. *J. Gen. Virol.* **2011**, *92*, 60.
- (a) Yamamoto, T.; Juneja, L. R.; Chu, D.-C.; Kim, M. *Chemistry and Applications of Green Tea*; CRC: Boca Raton, 1997; (b) Li, L.; Chan, T. H. *Org. Lett.* **2001**, *3*, 739.
- (a) Wan, S. B.; Dou, Q. P.; Chan, T. H. *Tetrahedron* **2006**, *62*, 5897; (b) Tanaka, H.; Miyoshi, H.; Chuang, Y.-C.; Ando, Y.; Takahashi, T. *Angew. Chem., Int. Ed.* **2007**, *46*, 5934.
- (a) Park, K. D.; Lee, S. G.; Kim, S. U.; Kim, S. H.; Sun, W. S.; Cho, S. J.; Jeong, D. H. *Bioorg. Med. Chem. Lett.* **2004**, *14*, 5189; (b) Anderson, J. C.; Headley, C.; Stapleton, P. D.; Taylor, P. W. *Bioorg. Med. Chem. Lett.* **2005**, *15*, 2633; (c) Hayes, C. J.; Whittaker, B. P.; Watson, S. A.; Grabowska, A. M. *J. Org. Chem.* **2006**, *71*, 9701; (d) Sánchez-del-Campo, L.; Otón, F.; Tárraga, A.; Cabezas-Herrera, J.; Chazarra, S.; Rodríguez-López, J. N. *J. Med. Chem.* **2008**, *51*, 2018.
- For several recent examples, see: (a) Hui, X.; Desrivort, J.; Bories, C.; Loiseau, P. M.; Franck, X.; Hocquemiller, R.; Figadère, B. *Bioorg. Med. Chem. Lett.* **2006**, *16*, 815; (b) Rong, F.; Chow, S.; Yan, S.; Larson, G.; Hong, Z.; Wu, J. *Bioorg. Med. Chem. Lett.* **2007**, *17*, 1663; (c) Zhang, L.; Qiu, B.; Xiong, B.; Li, X.; Li, J.; Wang, X.; Li, J.; Shen, J. *Bioorg. Med. Chem. Lett.* **2007**, *17*, 2118; (d) Porter, J.; Lumb, S.; Lecomte, F.; Reuberson, J.; Foley, A.; Calmiano, M.; Riche, K.; Edwards, H.;

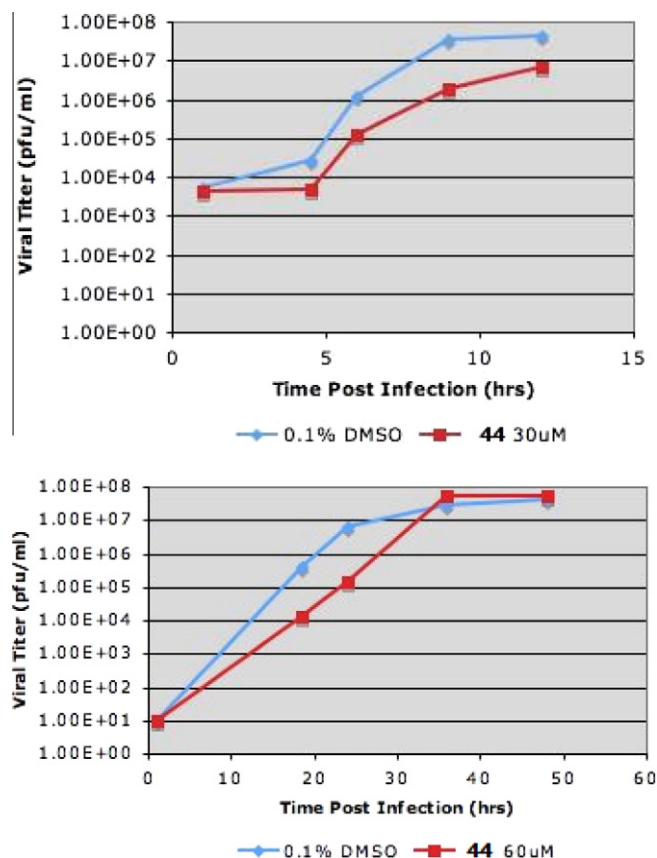


Figure 1. Single cycle virus growth curve (top panel) and multiple cycles virus growth curve (bottom panel) after compound 44 was incubated.

cycles growth curve at MOI 0.001 (bottom panel). Following 1 h infection, growth media containing compound 44 diluted in DMSO or control (0.1% DMSO) was added. Compound 44 inhibited influenza A/Udorn/72 virus growth \sim 10-fold (top panel). The multiple cycles growth assay indicates that compound 44 appeared to lose

- Delgado, J.; Franklin, R. J.; Gascon-Simorte, J. M.; Maloney, A.; Meier, C.; Batchelor, M. *Bioorg. Med. Chem. Lett.* **2009**, *19*, 397; (e) Romeiro, N. C.; Aguirre, G.; Hernández, P.; González, M.; Cerecetto, H.; Aldana, I.; Pérez-Silanes, S.; Monge, A.; Barreiro, E. J.; Lima, L. M. *Bioorg. Med. Chem.* **2009**, *17*, 641.
13. Liu, Y.; Sandoval, C. A.; Yamaguchi, Y.; Zhang, X.; Wang, Z.; Kato, K.; Ding, K. *J. Am. Chem. Soc.* **2006**, *128*, 14212.
14. (a) Chien, C.; Xu, Y.; Xiao, R.; Aramini, J. M.; Sahasrabudhe, P. V.; Krug, R. M.; Montelione, G. T. *Biochemistry* **2004**, *43*, 1950; (b) Rishi, V.; Potter, T.; Laudeman, J.; Reinhart, R.; Silvers, T.; Selby, M.; Stevenson, T.; Krosky, P.; Stephen, A. G.; Acharya, A.; Moll, J.; Oh, W. J.; Scudiero, D.; Shoemaker, R. H.; Vinson, C. *Anal. Biochem.* **2005**, *340*, 259.
15. Ar (in **23**, **24** and **25**) =

